IOPscience iopscience.iop.org

Home Search Collections Journals About Contact us My IOPscience

Multiple-scattering theory for clean superconducting layered structures

This article has been downloaded from IOPscience. Please scroll down to see the full text article.

2001 J. Phys.: Condens. Matter 13 8707

(http://iopscience.iop.org/0953-8984/13/38/312)

View the table of contents for this issue, or go to the journal homepage for more

Download details:
IP Address: 171.66.16.226
The article was downloaded on 16/05/2010 at 14:53

Please note that terms and conditions apply.

INSTITUTE OF PHYSICS PUBLISHING JOURNAL OF PHYSICS: CONDENSED MATTER

J. Phys.: Condens. Matter **13** (2001) 8707–8723 PII: S0953-8984(01)24871-1

Multiple-scattering theory for clean superconducting layered structures

R T W Koperdraad, R E S Otadoy[1], M Blaauboer and A Lodder[2]

Faculty of Sciences/Natuurkunde en Sterrenkunde, Vrije Universiteit, De Boelelaan 1081, 1081 HV Amsterdam, The Netherlands

E-mail: alod@nat.vu.nl (A Lodder)

Received 16 May 2001
Published 7 September 2001
Online at stacks.iop.org/JPhysCM/13/8707

Abstract

An exact expression is derived for the matrix Green's function of a clean superconducting layered structure with an arbitrary number of interfaces. A multiple-scattering approach is employed, in which the interfaces act as the scattering centres. Some initial applications of the theory to systems with transverse dimensions which vary from narrow to wide are given. The local density of states is calculated for an SNS and for an SNSNS junction ('S' standing for a superconducting layer and 'N' for a normal layer). For certain critical transverse widths the exact theory shows remarkable features not seen in the Andreev approximation. If the gap function for the systems is calculated self-consistently it turns out that for transverse dimensions smaller than twenty per cent of the superconducting coherence length, superconductivity is suppressed.

1. Introduction

Since the work of Gor'kov [1] and Bogoliubov *et al* [2], all basics have seemed to be available for a microscopic description of conventional superconductivity. However, practical applications of the theory, such as the calculation of the proximity effect in real inhomogeneous systems, are not straightforward at all. It is to the credit of Eilenberger [3] that he derived equations which are valid in the quasiclassical approximation and which are used extensively in present-day mesoscopic physics. The quasiclassical approximation amounts to the assumption that the gap energy Δ, which is the characteristic energy for superconducting phenomena, is much smaller than the Fermi energy or, equivalently, that the Fermi-electron wavelength is much smaller than the superconducting coherence length ξ. This assumption is a very good one for many applications.

[1] On leave of absence from: University of San Carlos, Nasipit, Talamban, Cebu City, Philippines.
[2] Author to whom any correspondence should be addressed.

 © 2001 IOP Publishing Ltd Printed in the UK

In clean systems, studied most intensively after the ballistic regime came within reach, Andreev reflection [4] is the predominant process in terms of which the properties are considered. The quasiclassical approximation for this process is equivalent to what is called the Andreev approximation [5]. Kümmel [6] was the first to point out that for an electron moving slowly in the direction of an N/S interface, and so having a relatively large transverse momentum, the Andreev approximation breaks down. In reflecting at the interface, not only is a hole reflected, retracing the path of the incoming electron, but also a non-negligible electron amplitude is reflected. While Kümmel worked out this idea for a superconducting layer with a thickness comparable to the superconducting coherence length, Šipr and Györffy [7] were the first to show explicitly its impact for a standard SNS junction.

It is the aim of the present paper to generalize the treatments available up to now in four ways. Firstly we derive a Green's-function description for junctions with an arbitrary number of interfaces. Previous calculations were based on extensions of the basic equation for the Green's function for specially chosen configurations [8] and the approach set out by Ishii [9] was followed. This approach is rather indirect and cumbersome, and the expressions obtained so far are not generally applicable. By developing a multiple-scattering formulation which is both transparent and flexible, these problems are overcome. The interfaces appear to be the scattering objects, whereas the quasiparticles propagate freely through the metals between the interfaces. Reflection and transmission processes are identified by scattering matrices. Our main result, equation (24) for the system T-matrix to be substituted in equation (20) for the system Green's function, has the basic structure of a multiple-scattering equation and clearly contains the t-matrix for scattering at a single interface.

Secondly, the formulation is devised in such a way that both exact results and results according to the Andreev approximation can be generated [8]. Thirdly, while Šipr and Györffy [7] just made a choice for the gap function Δ, we will give some results for a self-consistently calculated gap function. Finally, in addition to an SNS junction, a system with four instead of two interfaces will be treated; it is shown schematically in figure 1. Some preliminary results for an NS junction, not containing a self-consistent gap function yet, have been published by Blaauboer *et al* [10].

The paper is organized as follows. In section 2 the equation is given for the Green's function describing a system with an arbitrary number of interfaces. Subsequently, in the sections 3 and 4, two building blocks are constructed for this Green's function containing all multiple scattering. In section 3 an expression is given for the Green's function of a homogeneous system. In section 4 the Green's function describing scattering at a single interface is derived. The Green's function describing scattering by an arbitrary number of interfaces, accounting for all multiple scattering, is presented in section 5. In section 6 it is shown how differences in the chemical potential and interface potentials simulating possible imperfections of the contact planes can be accounted for easily. In section 7 the formalism is specified for an SNS′ junction, and some results are shown for an SNSNS junction as well. Self-consistent calculations of the gap function are presented in section 8. Finally, section 9 summarizes the conclusions.

2. The equation for the Green's function

The matrix Green's function satisfies the following differential equation [9]:

$$[\mathrm{i}\omega_n\tau_0 - K\tau_3 - D(x)]G(\boldsymbol{r},\boldsymbol{r}',\mathrm{i}\omega_n) = \delta(\boldsymbol{r}-\boldsymbol{r}')\tau_0 \tag{1}$$

where $G(\boldsymbol{r},\boldsymbol{r}',\mathrm{i}\omega_n)$ denotes the matrix Green's function, the grand-canonical Hamiltonian $K \equiv H - \mu$ is defined as the Hamiltonian minus the chemical potential μ, and

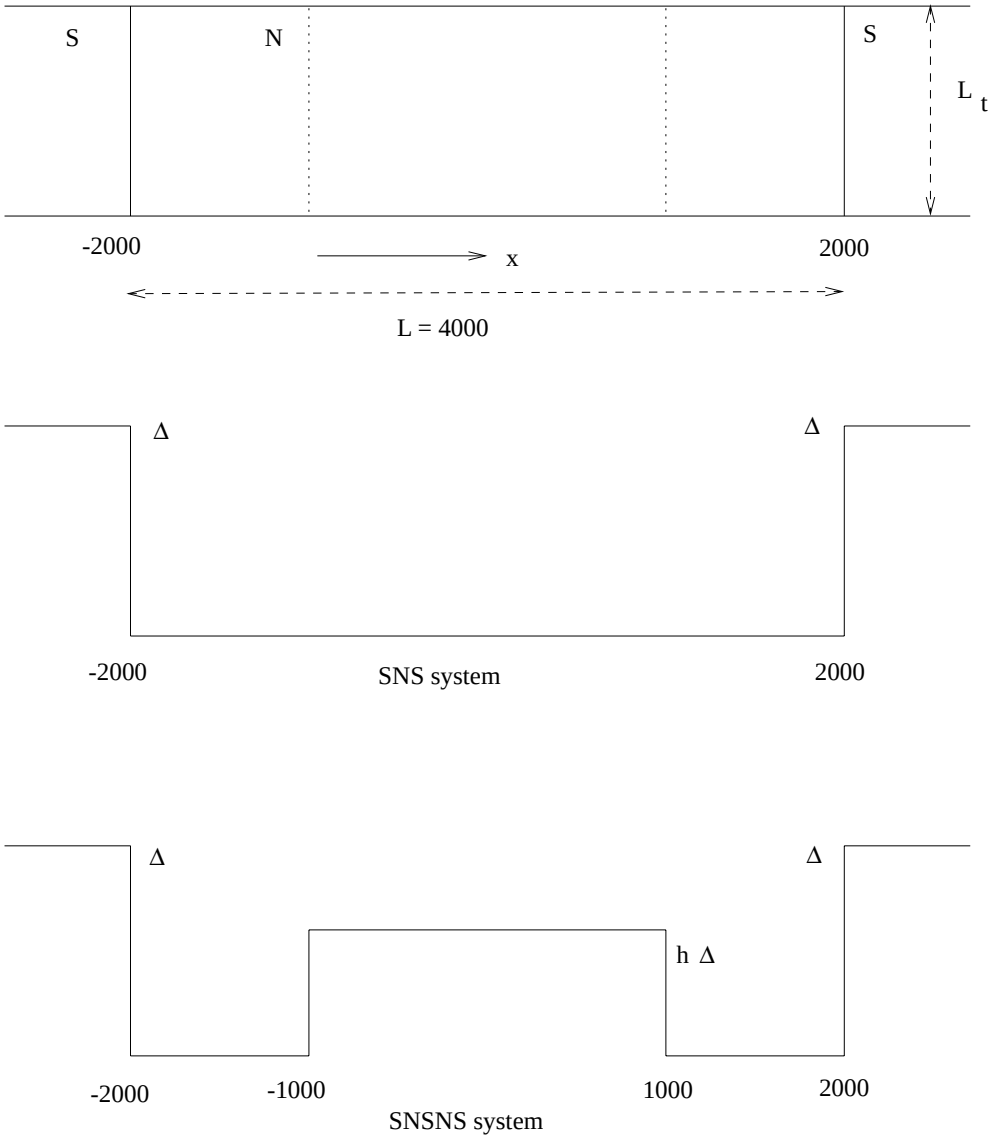

Figure 1. A two-dimensional picture of the systems studied. In the upper panel the vertical direction stands for a transverse direction. In the lower panels the potential is shown, which is zero in the normal part(s), and proportional to Δ in the superconducting parts.

$\omega_n = (2n + 1)\pi k_B T$ is the Matsubara frequency, T being the temperature. The matrices τ_0, τ_3, and $D(x)$ are given by

$$\tau_0 \equiv \begin{bmatrix} 1 & 0 \\ 0 & 1 \end{bmatrix} \qquad \tau_3 \equiv \begin{bmatrix} 1 & 0 \\ 0 & -1 \end{bmatrix} \qquad D(x) \equiv \begin{bmatrix} 0 & \Delta(x) \\ \Delta^*(x) & 0 \end{bmatrix} \tag{2}$$

where $\Delta(x)$ is the superconducting pair potential, which is modulated in the x-direction. One could look at figures 1 and 2 for examples of $\Delta(x)$, corresponding to SNS and SNSNS junctions and to the Kronig–Penney model respectively, the latter model representing an infinite multilayer [8].

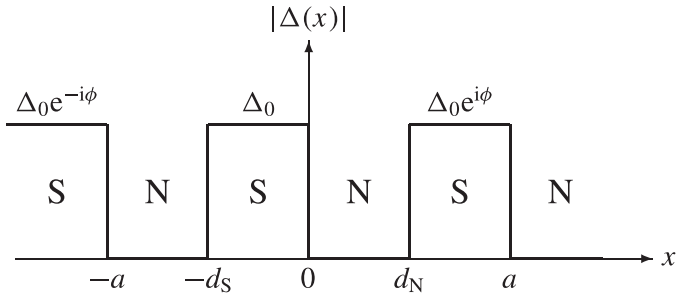

Figure 2. The Kronig–Penney model for the pair potential, used in reference [8].

The systems of interest are either translationally invariant or confined in the y- and z-directions. In the first case it is convenient to introduce the Fourier transform

$$G(x, x'; k_y, k_z, \mathrm{i}\omega_n) = \int G(\boldsymbol{r}, \boldsymbol{r}', \mathrm{i}\omega_n)\mathrm{e}^{-\mathrm{i}k_y(y-y')}\mathrm{e}^{-\mathrm{i}k_z(z-z')}\,\mathrm{d}y\,\mathrm{d}z \tag{3}$$

with respect to y and z. The transformed Green's function obeys

$$[\mathrm{i}\omega_n\tau_0 - K_x\tau_3 - D(x)]G(x, x'; k_y, k_z, \mathrm{i}\omega_n) = \delta(x - x')\tau_0 \tag{4}$$

where the grand-canonical Hamiltonian K_x is given by

$$K_x \equiv -\frac{\mathrm{d}^2}{\mathrm{d}x^2} - k_{Fx}^2 \qquad k_{Fx}^2 \equiv \mu - k_y^2 - k_z^2. \tag{5}$$

Atomic units are used in the sense that $\hbar = 2m = 1$. In the case of a confined system, to which the theory will be applied in the present paper, k_y and k_z are discrete. However, because the quasicontinuous k_y and k_z for the translationally invariant system are discrete as well, most expressions for the two cases are identical [10]. As is seen, the Hamiltonian does not contain a single-electron potential. It is essential for the treatment of clean systems that there is no impurity potential. In section 6 it will be shown that a modulated, but locally constant, potential can be subsumed in k_{Fx} simply, causing k_{Fx} to be modulated as well.

Observable properties can always be expressed in terms of the Green's function. In that sense, the Green's function contains all relevant information. An example of a quantity expressed in Green's functions is the pair potential itself, by means of the self-consistency condition

$$\Delta(x) = -k_B T V(x)\frac{1}{A_t}\sum_{k_y,k_z}\sum_n G_{12}(x, x; k_y, k_z, \mathrm{i}\omega_n) \tag{6}$$

in which G_{12} signifies the upper right element of the matrix Green's function G and A_t stands for the transverse cross section of the system. For an infinite system, A_t becomes infinity and the summations over k_y and k_z become integrals in the usual way. Another example comes from Tanaka and Tsukada [8], who computed supercurrent densities from the Green's function by means of the formula

$$I = -\frac{\mathrm{i}e}{A_t}\sum_{k_y,k_z}\lim_{x'\to x}\left(\frac{\partial}{\partial x'} - \frac{\partial}{\partial x}\right)k_B T\sum_n G_{11}(x, x'; k_y, k_z, \mathrm{i}\omega_n) \tag{7}$$

where G_{11} signifies the upper left element of the matrix Green's function G. Note that both equations (6) and (7) require a nontrivial summation over the Matsubara frequencies. The local quasiparticle density of states (LDOS) is given by

$$\rho(x, \epsilon) = -\frac{1}{\pi}\lim_{\delta\to 0}\frac{1}{A_t}\sum_{k_y,k_z}\mathrm{Im}\,G_{11}(x, x; k_y, k_z, \epsilon + \mathrm{i}\delta). \tag{8}$$

For this equation, the analytical continuation of the temperature Green's function is used. It is obtained simply by making the replacement $i\omega_n \to \epsilon + i\delta$, with $\omega_n > 0$.

3. The Green's function for the homogeneous superconductor

The solution of equation (4) for a homogeneous superconductor is easily written down [9]. Assuming a constant pair potential $\Delta(x) = \Delta_S e^{i\phi_S}$, denoting the corresponding $D(x)$ by the constant D_S, denoting G for this special case by $\mathcal{G}_S$, and suppressing in it the dependence on k_y, k_z, and $i\omega_n$, the result reads as

$$\mathcal{G}_S(x, x') = \sum_\sigma \mathcal{G}_S^\sigma(x, x') \tag{9a}$$

$$\mathcal{G}_S^\sigma(x, x') = d_S^\sigma M_S^\sigma e^{i\sigma k_S^\sigma |x-x'|} \tag{9b}$$

$$k_S^\sigma = \operatorname{sgn}\omega_n \sqrt{k_{Fx}^2 + i\sigma\Omega_S} \qquad \operatorname{Im}\sigma k_S^\sigma > 0 \tag{9c}$$

$$i\Omega_S = \sqrt{(i\omega_n + 0^+)^2 - \Delta_S^2} \tag{9d}$$

$$M_S^\sigma = i\omega_n\tau_0 + i\sigma\Omega_S\tau_3 + D_S \tag{9e}$$

$$d_S^\sigma = -\frac{1}{4\Omega_S k_S^\sigma}. \tag{9f}$$

The upper index σ is ± 1 and the summation in equation (9a) runs over both possibilities. The condition for the imaginary part of k_S^σ guarantees the convergence of $\mathcal{G}_S(x, x')$ when one of the coordinates approaches infinity. The infinitesimally positive quantity 0^+ in equation (9d) is added to ensure that $i\Omega_S \to i\omega_n$ in the case where Δ_S vanishes. This implies that $\operatorname{sgn}\Omega_S = \operatorname{sgn}\omega_n$. When $\mathcal{G}_S(x, x')$ is substituted in equation (4), the dependence on $|x - x'|$ in equation (9b) leads to the δ-function on the right-hand side and the equation is satisfied.

A particularly clear way of expressing the Green's function is obtained by means of the solutions of the differential equation

$$[i\omega_n\tau_0 - K_x\tau_3 - D(x)]\psi_S^{\sigma\nu}(x) = 0. \tag{10}$$

This is, in fact, the Bogoliubov equation [8] with an imaginary eigenvalue $i\omega_n$. Note that a Hermitian operator can have complex eigenvalues, as long as no boundary conditions are applied to the wave functions $\psi_S{}^{\sigma\nu}(x)$. It is easily checked that the solutions read as

$$\psi_S^{\sigma\nu}(x) = \begin{bmatrix} u_S^\sigma e^{i\phi_S/2} \\ u_S^{-\sigma} e^{-i\phi_S/2} \end{bmatrix} e^{i\sigma\nu k_S^\sigma x} \tag{11}$$

with

$$u_S^\sigma = \sqrt{i\omega_n + i\sigma\Omega_S}$$

(note that $u_S^\sigma u_S^{-\sigma} = \Delta_S$). The four standard solutions are labelled with the sign indices σ and ν, which can both take the values ± 1. Obviously, these can be related to the solutions of the ordinary Bogoliubov equation [8] by making the substitution $i\omega_n \to \epsilon$. We then obtain wave functions whose index σ refers to the type of the propagating particle (electronlike for $\sigma = +$ and holelike for $\sigma = -$) and whose index ν indicates the direction of propagation.

In order to express the Green's function in terms of $\psi_S^{\sigma\nu}(x)$, a conjugate wave function is needed, namely,

$$\tilde{\psi}_S^{\sigma\nu}(x) = \begin{bmatrix} u_S^\sigma e^{-i\phi_S/2} & u_S^{-\sigma} e^{i\phi_S/2} \end{bmatrix} e^{i\sigma\nu k_S^\sigma x} \tag{12}$$

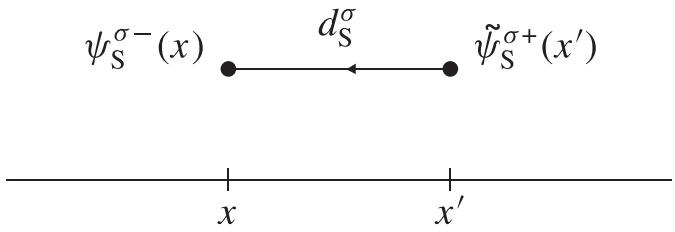

Figure 3. The free propagation of a quasiparticle. Summation over σ yields the Green's function of a homogeneous superconductor .

(which is not the *Hermitian* conjugate). Unlike the original wave function, ν has now to be explained as minus the direction of propagation. This is necessary to arrive at a consistent interpretation in multiple-scattering language. Using equations (11) and (12), one can write the σ-dependent Green's function parts, equation (9*b*), as follows:

$$\mathcal{G}_S^\sigma(x,x') = d_S^\sigma \psi_S^{\sigma-}(x_<)\tilde{\psi}_S^{\sigma+}(x_>) = d_S^\sigma \psi_S^{\sigma+}(x_>)\tilde{\psi}_S^{\sigma-}(x_<) \tag{13}$$

where $x_>$ ($x_<$) denotes the largest (smallest) coordinate of x and x'. From the similarity of equations (4) and (10), it is immediately seen that expression (13) satisfies equation (4) when $x \neq x'$. The singularity in equation (13) at $x = x'$ ensures that the δ-function on the right-hand side of equation (4) appears.

It is illuminating to adopt the following interpretation of the Green's function $\mathcal{G}_S^\sigma(x,x')$, which is shown in figure 3. Assume that $x < x'$. The Green's function can then be expressed in terms of $d_S^\sigma \psi_S^{\sigma-}(x)\tilde{\psi}_S^{\sigma+}(x')$. In this form, it describes the propagation of a particle travelling from x' to x. The particle is either electronlike ($\sigma = +1$) or holelike ($\sigma = -1$). The second index of the first wave function indicates where the particle is going to—in this example to the negative side, because $x < x'$. The second index of the conjugate function indicates where the particle is coming from—in this example, the positive side. The direction of motion in x' is minus the second index of the conjugate wave function $\tilde{\psi}_S^{\sigma+}(x')$. The total Green's function $\mathcal{G}_S(x,x')$ is the sum of the two possible ways to propagate from x' to x, namely, either as an electronlike or as a holelike particle. Depending on σ, figure 3 shows the electronlike or holelike term of the Green's function (9*a*). Each term consists of a contribution $\tilde{\psi}_S^{\sigma+}(x')$ for the departing quasiparticle, a contribution $\psi_S^{\sigma-}(x)$ for the arriving quasiparticle, and a factor d_S^σ for the propagation. It is a general feature of a Green's function that it can be written as the sum over all processes in which the two coordinates are connected by the propagation of a particle through the system.

As soon as boundary conditions are concerned it is convenient to extend the two-component vectors (11) and (12) to four-component vectors by including the derivatives of the wave functions. For example, instead of equation (11) we use

$$\psi_S^{\sigma\nu}(x) \equiv \begin{bmatrix} u_S^\sigma e^{i\phi_S/2} \\ u_S^{-\sigma} e^{-i\phi_S/2} \\ i\sigma\nu k_S^\sigma u_S^\sigma e^{i\phi_S/2} \\ i\sigma\nu k_S^\sigma u_S^{-\sigma} e^{-i\phi_S/2} \end{bmatrix} e^{i\sigma\nu k_S^\sigma x}. \tag{14}$$

The boundary conditions then simply require the continuity of all four components. Below, it will be implicitly assumed that the wave functions are four-component vectors. This makes the Green's function (13) a 4×4 matrix, of which the upper left quarter is the actual 2×2 matrix Green's function.

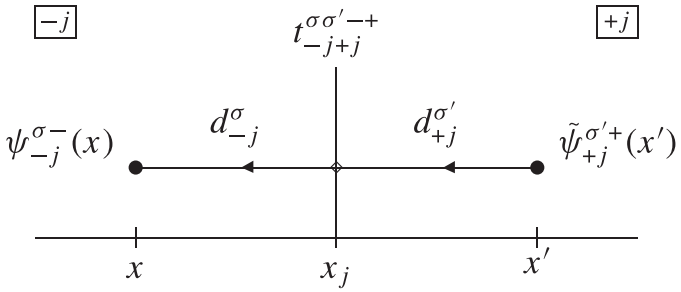

Figure 4. The propagation of a quasiparticle in a system with two half-infinite pieces of metal joined by a single interface. x and x' are on different sides. Summation over σ and σ' yields the Green's function $G_{-j+j}(x, x')$.

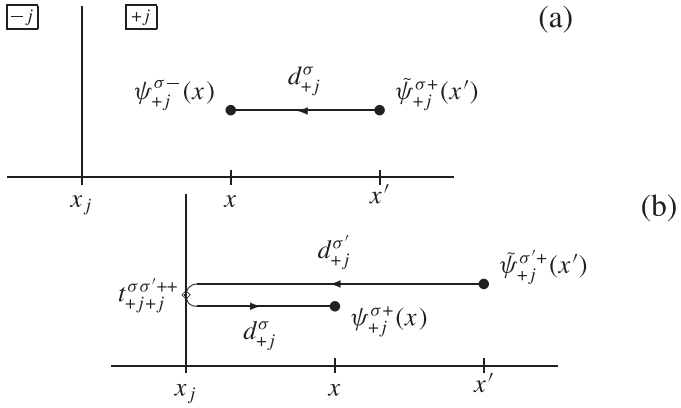

Figure 5. The propagation of a quasiparticle in a system with two half-infinite pieces of metal joined by a single interface. x and x' are on the same side. The propagation can be direct (a) or via the interface (b). (a) summed over σ plus (b) summed over σ and σ' yields the Green's function $G_{+j+j}(x, x')$.

4. The Green's function accounting for scattering at a single interface

The first step towards the discussion of arbitrary layered structures is the analysis of a system with two half-infinite pieces of metal separated by a single interface. Let x_j be the position of the interface. One can infer from equations (4) and (10) that the general form of the Green's function should be

$$G_{\nu j\nu' j}(x, x') = \mathcal{G}_{\nu j}(x, x')\delta_{\nu\nu'} + \sum_{\sigma\sigma'} d^{\sigma}_{\nu j} d^{\sigma'}_{\nu' j} \psi^{\sigma\nu}_{\nu j}(x) t^{\sigma\sigma'\nu\nu'}_{\nu j\nu' j} \tilde{\psi}^{\sigma'\nu'}_{\nu' j}(x') \tag{15}$$

where, according to equations (9*a*) and (13),

$$\mathcal{G}_{\nu j}(x, x') = \sum_{\sigma} d^{\sigma}_{\nu j} \psi^{\sigma\mu}_{\nu j}(x) \tilde{\psi}^{\sigma,-\mu}_{\nu j}(x') \tag{16}$$

where

$$\mu = \operatorname{sgn}(x - x').$$

All subscripts are material indices and serve to indicate the different parts of the system, just as the subscript S referred to the superconductor in the previous equations. The following indexing has been adopted (see also figures 4 and 5). For $\mathcal{G}_{\nu j}(x, x')$, $d^{\sigma}_{\nu j}$, $\psi^{\sigma\nu}_{\nu j}(x)$, and

$\tilde{\psi}^{\sigma\nu}_{\nu j}(x)$, the subscript (νj) refers to the part of the system that is on the ν-side of the interface with position x_j. Since there is only a single interface, $(-j)$ refers to the material to the left of x_j, whereas $(+j)$ refers to the material to the right of the interface. For $G_{\nu j\nu' j'}(x, x')$, the unprimed and primed indices apply in the same way to the positions of x and x', respectively. So, for example, $G_{+j+j}(x, x')$ is only defined for both x and x' to the right of the interface j.

The first term in equation (15) is fully responsible for the appearance of the δ-function in equation (4). So to satisfy equation (4), the second term should be continuous and have a continuous derivative. The first term accounts for the possible ways of propagating from x' to x without being scattered at the interface; see figure 5(a). The second term describes the propagation via the interface; see figures 4 and 5(b). The reflection and transmission processes are described by the scattering matrix $t^{\sigma\sigma'\nu\nu'}_{\nu j\nu' j}$. It refers to the process where a σ'-particle is incident from the ν'-side of the interface. After being scattered it has been changed to a σ-particle and leaves the interface on the ν-side. During the scattering process the particle can change its type, so the possibility of Andreev reflection is incorporated in the formulation. The fact that the wave functions have the same upper right and lower left indices takes care of the convergence of the Green's function at plus and minus infinity. This reflects the notion that in the present case of a single interface a particle can be scattered only once. Therefore, the directions of motion of the incident and scattered particles are coupled to the positions ν and ν' of x and x' with respect to the interface.

Figure 5 shows the relevant processes in the expansion of $G_{+j+j}(x, x')$. Figure 5(a) shows the two free propagations from x' to x ($\sigma = \pm 1$). These terms are constructed in the same way as was done for figure 3. Figure 5(b) shows the four possible reflections connecting x' to x ($\sigma = \pm 1$, $\sigma' = \pm 1$). These terms consist of a conjugate wave function for the point of departure, a wave function for the point of arrival, two factors $d^{\sigma}_{\nu j}$ and $d^{\sigma'}_{\nu' j}$ for the two propagations, and a scattering matrix $t^{\sigma\sigma'\nu\nu'}_{\nu j\nu' j}$ for the reflection. Similarly, figure 4 is the visualization of $G_{-j+j}(x, x')$.

The present way of writing the general solution is somewhat different from the path followed by Ishii [9]. By introducing the matrices $T^{\sigma,\sigma'}$ in the way that Ishii does in *his* equation (2.12), the problem is underdetermined. He has to impose additional restrictions on the matrices to arrive at a well-defined problem. This is done in *his* equation (2.21). This procedure is not very elegant and is avoided in the present treatment. Furthermore, his usage of integral equations requires the evaluation of complex integrals. This is another thing that can be avoided, as is shown in the present treatment.

The scattering matrix $t^{\sigma\sigma'\nu\nu'}_{\nu j\nu' j'}$ is found by applying the boundary conditions. The present method of indexing allows for a very compact notation. The condition for $x = x_j$ reads as

$$\sum_{\nu} \nu G_{\nu j\nu' j}(x_j, x') = 0 \qquad (\forall x'). \tag{17}$$

It is sufficient to impose the boundary condition on the first coordinate only. This leads to a closed set of equations. Due to the special form of equation (15), applying the boundary condition to the second coordinate would yield the same equations. When $x = x_j$ it is known that x' is situated on the ν'-side of x and that consequently $\mu = -\nu'$, so equation (15) with equation (16) can be written as

$$G_{\nu j\nu' j}(x_j, x') = \sum_{\sigma'} d^{\sigma'}_{\nu' j}\left(\psi^{\sigma';-\nu'}_{\nu' j}(x_j)\delta_{\nu\nu'} + \sum_{\sigma} d^{\sigma}_{\nu j}\psi^{\sigma\nu}_{\nu j}(x_j)t^{\sigma\sigma'\nu\nu'}_{\nu j\nu' j}\right)\tilde{\psi}^{\sigma'\nu'}_{\nu' j}(x'). \tag{18}$$

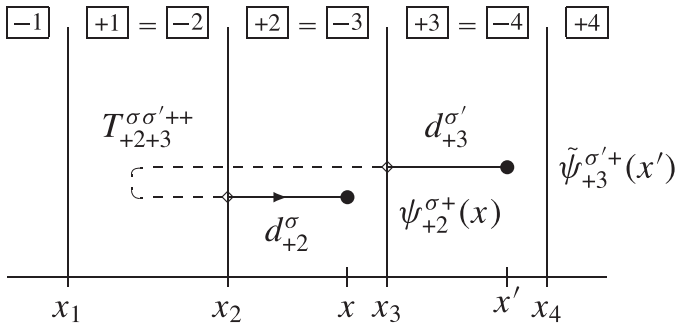

Figure 6. The propagation of a particle through a layered system. The dashed line represents an example of a multiple-scattering process. The boxes at the top contain the layer indices.

Substituting this expression into the boundary condition and using the linear independence of the four conjugate wave functions (12), the boundary condition changes into

$$\sum_{\sigma\nu} \nu d^{\sigma}_{\nu j} \psi^{\sigma\nu}_{\nu j}(x_j) t^{\sigma\sigma'\nu\nu'}_{\nu j\nu' j} = -\nu' \psi^{\sigma',-\nu'}_{\nu' j}(x_j) \qquad (\forall\sigma', \nu'). \tag{19}$$

This is a well-defined set of equations for the t-matrix elements. The solution is found by regarding $t^{\sigma\sigma'\nu\nu'}_{\nu j\nu' j}$ and $\psi^{\sigma\nu}_{\nu j}(x_j)$ as 4×4 matrices. The first has row index (σ, ν) and column index (σ', ν'). The second has column index (σ, ν), whereas the four components of $\psi^{\sigma\nu}_{\nu j}(x_j)$ fill up the four rows.

5. The Green's function for scattering at multiple interfaces

Consider a system with an arbitrary number of interfaces j, with position coordinates $x_j < x_{j+1}$. The scattering of the quasiparticles will be described in terms of the scattering matrices $T^{\sigma\sigma'\mu\mu'}_{\nu j\nu' j'}$. The meaning of the indices is the same as before: a σ'-particle is coming from the μ'-direction through the part of the system on the ν'-side of the interface j'. After an arbitrary number of scattering processes, it ends up as a σ-particle travelling in the μ-direction through the part of the system on the ν-side of the interface j.

This is illustrated in figure 6 for $T^{\sigma\sigma'++}_{+2+3}$, where the dashed line is used to signify the multiple-scattering process. In accordance with this interpretation, the general form of the Green's function is

$$\begin{aligned} G_{\nu j\nu' j'}(x, x') &= \mathcal{G}_{\nu j}(x, x')[\delta_{\nu\nu'}\delta_{jj'} + \delta_{-\nu\nu'}\delta_{j+\nu, j'}] \\ &\quad + \sum_{\sigma\sigma'} \sum_{\mu\mu'} d^{\sigma}_{\nu j} d^{\sigma'}_{\nu' j'} \psi^{\sigma\mu}_{\nu j}(x) T^{\sigma\sigma'\mu\mu'}_{\nu j\nu' j'} \tilde{\psi}^{\sigma'\mu'}_{\nu' j'}(x'). \end{aligned} \tag{20}$$

The first term is more complicated than in equation (15). The reason for this is that there is a redundancy in the indexing of various parts of the system. A layer indicated by, for example, $(\nu j) = (+j)$ can equally well be indicated by $(-\nu, j + \nu) = (-, j + 1)$. The first combination addresses the layer to the right of the jth interface, whereas the latter indicates the layer to the left of the $(j + 1)$th interface. Obviously, these layers are the same. A second difference from equation (15) is that the second term contains extra summations over μ and μ'. The reason for this is that the convergency conditions for the Green's function cease to apply for the inner layers. The particle can be scattered many times. In inner layers, it can leave x' in either direction and in the end nevertheless arrive at x. Similarly, in inner layers, it can

reach x from either direction. Of course, in the outer two half-infinite parts of the system the Green's function must converge. When $j_{\min}$ and $j_{\max}$ are the leftmost and rightmost interfaces, respectively, the boundary conditions at infinity require that

$$T^{\sigma\sigma'\mu+}_{\nu j,-j_{\min}} = T^{\sigma\sigma'\mu-}_{\nu j,+j_{\max}} = T^{\sigma\sigma'+\mu'}_{-j_{\min},\nu' j'} = T^{\sigma\sigma'-\mu'}_{+j_{\max},\nu' j'} = 0.$$

As for the single interface, the boundary condition for $x = x_j$ is

$$\sum_{\nu} \nu G_{\nu j\nu' j'}(x_j, x') = 0 \qquad (\forall x' \text{and} \forall \nu', j'). \tag{21}$$

From equations (20) and (16) it is seen that

$$G_{\nu j\nu' j'}(x_j, x') = \sum_{\sigma'\mu'} d^{\sigma'}_{\nu' j'} \Bigg(\psi^{\sigma',-\mu'}_{\nu j}(x_j)\delta_{\mu'\nu}[\delta_{\nu\nu'}\delta_{jj'} + \delta_{-\nu\nu'}\delta_{j+\nu,j'}] + \sum_{\sigma\mu} d^{\sigma}_{\nu j}\psi^{\sigma\mu}_{\nu j}(x_j) T^{\sigma\sigma'\mu\mu'}_{\nu j\nu' j'} \Bigg) \tilde{\psi}^{\sigma'\mu'}_{\nu' j'}(x'). \tag{22}$$

Substituting this, and writing out the summation over μ for $\mu = \pm\nu$, one finds from condition (21) for the T-matrices that

$$\sum_{\sigma\nu} \nu d^{\sigma}_{\nu j}\psi^{\sigma\nu}_{\nu j}(x_j) T^{\sigma\sigma'\nu\mu'}_{\nu j\nu' j'} = -\mu'\psi^{\sigma',-\mu'}_{\mu' j}(x_j)[\delta_{\mu'\nu'}\delta_{jj'} + \delta_{-\mu'\nu'}\delta_{j+\mu',j'}] + \sum_{\sigma\nu} -\nu d^{\sigma}_{\nu j}\psi^{\sigma,-\nu}_{\nu j}(x_j) T^{\sigma\sigma',-\nu\mu'}_{\nu j\nu' j'} \qquad (\forall\sigma', \mu'). \tag{23}$$

By use of the implicit solutions of equation (19) it can be turned into the familiar form of a Lippmann–Schwinger equation:

$$T^{\sigma\sigma'\nu\mu'}_{\nu j\nu' j'} = t^{\sigma\sigma'\nu\mu'}_{\nu j\mu' j}[\delta_{\mu'\nu'}\delta_{jj'} + \delta_{-\mu'\nu'}\delta_{j+\mu',j'}] + \sum_{\sigma''\nu''} t^{\sigma\sigma''\nu\nu''}_{\nu j\nu'' j} d^{\sigma''}_{\nu'' j} T^{\sigma''\sigma',-\nu''\mu'}_{\nu'' j\nu' j'}. \tag{24}$$

This equation, together with equation (20), forms the main result of the present paper. The idea of multiple scattering shows up clearly in equation (24). The matrix $T^{\sigma\sigma'\nu\mu'}_{\nu j\nu' j'}$ is found by adding all possible processes that yield the correct final state. The first term in equation (24) accounts for the possibility that the particle is scattered once. The second term collects the processes in which the particle is scattered once due to $t^{\sigma\sigma''\nu\nu''}_{\nu j\nu'' j}$ and an arbitrary number of other times due to $T^{\sigma''\sigma',-\nu''\mu'}_{\nu'' j\nu' j'}$.

Figure 7 shows how figure 6 develops on applying equation (24) to $T^{\sigma\sigma'++}_{+2+3}$. Figure 7(a) shows the processes that end with a transmission ($\nu'' = -\nu$). Figure 7(b) shows the processes that end with a reflection ($\nu'' = \nu$).

Repeated application of equation (24) reveals the correct multiplication rules for the t-matrices. An example of a correct sequence is

$$t^{\sigma\sigma'-\nu\nu'}_{-\nu j\nu' j} d^{\sigma'}_{\nu' j} t^{\sigma'\sigma'',-\nu'\nu''}_{-\nu',j+\nu',\nu'',j+\nu'} d^{\sigma''}_{\nu'',j+\nu'} t^{\sigma''\sigma''',-\nu''\nu'''}_{-\nu'',j+\nu'+\nu'',\nu''',j+\nu'+\nu''} \cdots.$$

The outgoing-particle type of one t-matrix has to equal the incoming-particle type of the next t-matrix. However, when a scattering process ends with a particle travelling *in* the ν-direction, the next scattering will start with a particle coming *from* the $-\nu$-direction. The lower indices, which indicate the different parts of the system, have to match the geometry of the system.

6. Locally constant and interface barrier potentials

It was mentioned below equation (5) that a modulated, but locally constant potential can be accounted for by taking it into the definition of the one-dimensional Fermi wave vector:

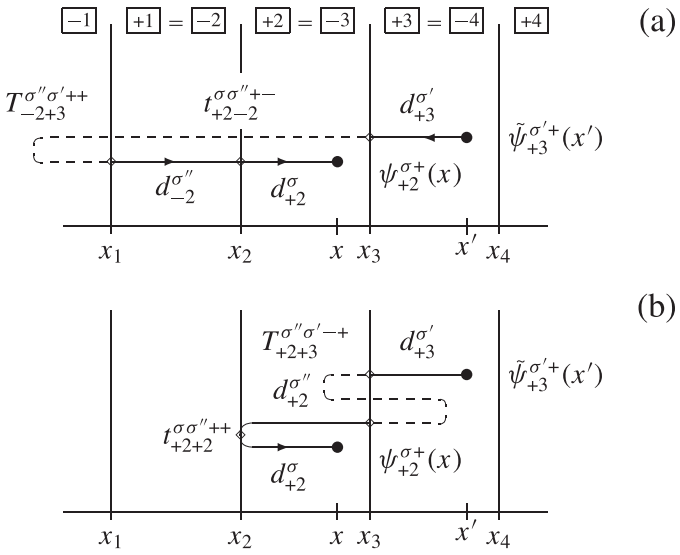

Figure 7. A schematic representation of equation (24). Summation over σ'' of diagrams (a) and (b) yields the diagram of figure 6.

$k^2_{Fx}(x) \equiv \mu - k_y^2 - k_z^2 - V(x)$. It is also easy to account for δ-potentials at the interfaces. Assume that the grand-canonical Hamiltonian reads as

$$K_x \equiv -\frac{\mathrm{d}^2}{\mathrm{d}x^2} - k^2_{Fx} + \sum_j V_j \delta(x - x_j). \tag{25}$$

The four-component standard solutions are still given by equation (14), but the matrix Green's function built up with them is subject to different boundary conditions. Instead of equation (17) one has

$$\sum_\nu S_{\nu j} G_{\nu j \nu' j}(x_j, x') = 0 \tag{26}$$

where

$$S_{\nu j} \equiv \begin{bmatrix} \nu & 0 & 0 & 0 \\ 0 & \nu & 0 & 0 \\ -\frac{1}{2}V_j & 0 & \nu & 0 \\ 0 & -\frac{1}{2}V_j & 0 & \nu \end{bmatrix}. \tag{27}$$

One can check that this corresponds to the more familiar conditions for the 2×2 matrix Green's function:

$$G_{+j\nu' j}(x_j, x') = G_{-j\nu' j}(x_j, x') \tag{28a}$$

$$\frac{\mathrm{d}}{\mathrm{d}x} G_{+j\nu' j}(x_j, x')\bigg|_{x=x_j} = \frac{\mathrm{d}}{\mathrm{d}x} G_{-j\nu' j}(x_j, x')\bigg|_{x=x_j} + V_j G_{-j\nu' j}(x_j, x'). \tag{28b}$$

Expanding equation (26), one finds

$$\sum_{\sigma\nu} d^\sigma_{\nu j} S_{\nu j} \psi^{\sigma\nu}_{\nu j}(x_j) t^{\sigma\sigma'\nu\nu'}_{\nu j \nu' j} = -S_{\nu' j} \psi^{\sigma';-\nu'}_{\nu' j}(x_j) \tag{29}$$

which takes the place of equation (19). Because equations (21) and (23) must be adapted similarly, equation (24) remains unaltered. The whole of the remaining analysis holds in the presence of interface potentials. Note also that the matrices $S_{\nu j}$ and $U(\phi_{\nu j})$ commute.

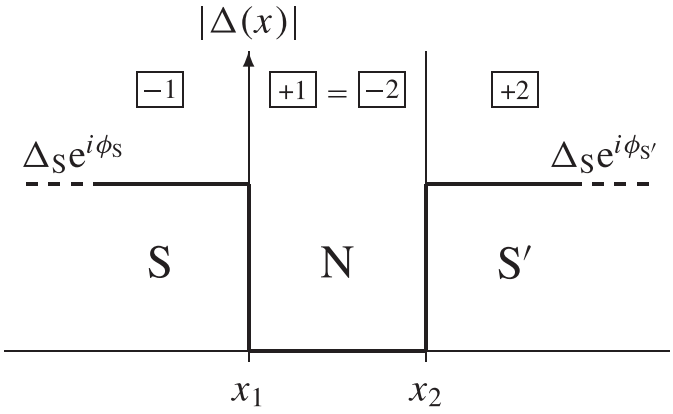

Figure 8. The pair potential in an SNS junction. The boxes at the top contain the general layer indices. The indices S, N, and S′ are specific to the SNS junction configuration.

7. The local density of states in SNS and SNSNS junctions

As an introduction to some results for the local density of states it is instructive to work out equation (24) for a system with two interfaces, as shown in figure 8.

One can remove the redundancy in the layer indexing by requiring that $\nu = \mu$ and $\nu' = \mu'$ in each T-matrix $T^{\sigma\sigma'\mu\mu'}_{\nu j\nu' j'}$. This can be done without loss of generality. The indices ν and ν' are then completely fixed and a single, unequivocal choice is left for the interface indices j and j'. Equation (24) now simplifies to

$$T^{\sigma\sigma'\nu\nu'}_{\nu j\nu' j'} = t^{\sigma\sigma'\nu\nu'}_{\nu j\nu' j}\delta_{jj'} + \sum_{\sigma''\nu''} t^{\sigma\sigma'',\nu\nu''}_{\nu j\nu'' j} d^{\sigma''}_{\nu'' j} T^{\sigma''\sigma',-\nu''\nu'}_{-\nu'',j+\nu'',\nu' j'} \tag{30}$$

where we used $(\nu'' j) = (-\nu'', j + \nu'')$. The convergence of the Green's function requires that $T^{\sigma''\sigma',-\nu''\mu'}_{-\nu'',j+\nu'',\nu' j'}$ vanishes when $j + \nu''$ is a nonexistent interface. It is convenient to substitute $-\nu$ for ν, so that all sequences of upper indices take on the same form. Doing this and using the fact that there are only two interfaces, equation (30) can be expanded, yielding

$$\begin{bmatrix} T^{\sigma\sigma',-\nu\nu'}_{-\nu 1\nu' 1} & T^{\sigma\sigma',-\nu\nu'}_{-\nu 1\nu' 2} \\ T^{\sigma\sigma',-\nu\nu'}_{-\nu 2\nu' 1} & T^{\sigma\sigma',-\nu\nu'}_{-\nu 2\nu' 2} \end{bmatrix} = \begin{bmatrix} t^{\sigma\sigma',-\nu\nu'}_{-\nu 1\nu' 1} & 0 \\ 0 & t^{\sigma\sigma',-\nu\nu'}_{-\nu 2\nu' 2} \end{bmatrix}$$
$$+ \sum_{\sigma''\nu''} \begin{bmatrix} 0 & t^{\sigma\sigma'',-\nu\nu''}_{-\nu 1\nu'' 1} d^{\sigma''}_{\nu'' 1}\delta_{\nu''+} \\ t^{\sigma\sigma'',-\nu\nu''}_{-\nu 2\nu'' 2} d^{\sigma''}_{\nu'' 2}\delta_{\nu''-} & 0 \end{bmatrix} \begin{bmatrix} T^{\sigma''\sigma',-\nu''\nu'}_{-\nu''1\nu' 1} & T^{\sigma''\sigma',-\nu''\nu'}_{-\nu''1\nu' 2} \\ T^{\sigma''\sigma',-\nu''\nu'}_{-\nu''2\nu' 1} & T^{\sigma''\sigma',-\nu''\nu'}_{-\nu''2\nu' 2} \end{bmatrix}. \tag{31}$$

Instead of using 2×2 matrices and writing out the summation over σ'' and ν'', one can regard each matrix as an 8×8 matrix with the sign indices as extra labels. All 64 T-matrix elements are then grouped in an 8×8 matrix, which obeys an equation that is easily solved. There is no problem in extending the procedure to an arbitrary, but finite number of interfaces. This is simply done by making the matrices in the Lippmann–Schwinger equation correspondingly larger. The solution is always found by a straightforward matrix inversion.

Applications of the general equation (24) to an arbitrary multilayer, a periodic multilayer, or a current-carrying multilayer will not be given explicitly in the present paper, but the interested reader can find them in Koperdraad's PhD Thesis [11]. The same holds for the simplifications achieved by applying the frequently used Andreev approximation.

We conclude by showing some applications to an SNS and an SNSNS system, depicted schematically in figure 1. The system length L has been chosen to be of the same order of magnitude as in the work of Blaauboer *et al* [10], and for the applications of the theory in the present section it is equal to 4000 Bohr. The system width of the bar-shaped system, with $L_y = L_z = L_t$, has been chosen much more critically, such that the highest transverse mode has the smallest longitudinal momentum which still allows for propagation. It is determined by the gap Δ and the Fermi energy μ, chosen to be equal to 0.0001 Ryd and 0.5 Ryd. If one requires that only the (0, 0), (0, 1), and (1, 0) modes propagate, L_t follows from the condition $\pi^2/L_t^2 = \mu - \Delta = 0.4999$ Ryd for the maximum transverse mode energy. This leads to $L_t = 4.4438$. If one allows for propagation of one more mode, the (1, 1) mode, one finds according to $2\pi^2/L_t^2 = 0.4999$ Ryd that $L_t = 6.2838$ Bohr. The local density of states (LDOS) is calculated using

$$\mathrm{LDOS}(x, E) = -\frac{1}{\pi L_y L_z} \lim_{\delta \to 0} \sum_{k_y, k_z} \mathrm{Im}\, G_{11}(x, x; k_y, k_z, E + \mathrm{i}\delta) \tag{32}$$

which is the finite-transverse-size version of equation (8). In figure 9 the LDOS is shown for $L_t = 6.2838$ at $x = -1500$ Bohr. Both the states according to the Andreev approximation (AA) and the exact states are shown, using a small but not negligible energy width δ. One clearly sees the nice set of equidistant AA states corresponding to the highest mode, the (1, 1) mode, and the splitting in the exact case. The two states corresponding to the (0, 0) and degenerate (0, 1) and (1, 0) modes lie just below the gap and can be recognized as shoulders of the highest peaks. The peaks for the exact states have different heights, which is directly related to the choice of the position x and reflects the fact that the LDOS is proportional to the absolute square

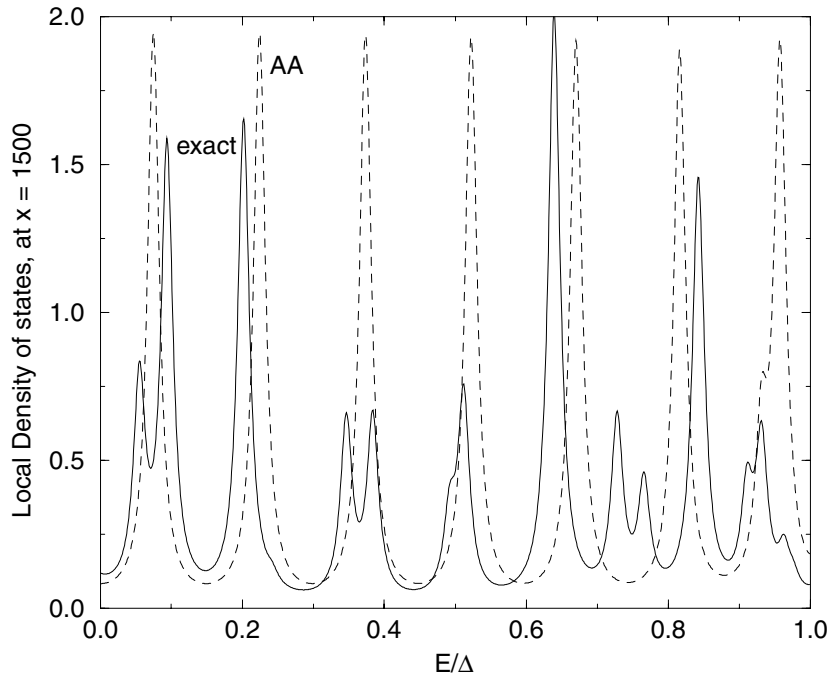

Figure 9. A plot of the LDOS at $x = -1500$ Bohr against the ratio of the quasiparticle excitation energy E to the gap Δ, for the SNS system depicted in figure 1, with $L_t = 6.2838$ Bohr, $L = 4000$ Bohr, and $\Delta = 0.0001$ Ryd. The solid and broken curves represent the exact calculation and the Andreev approximation respectively.

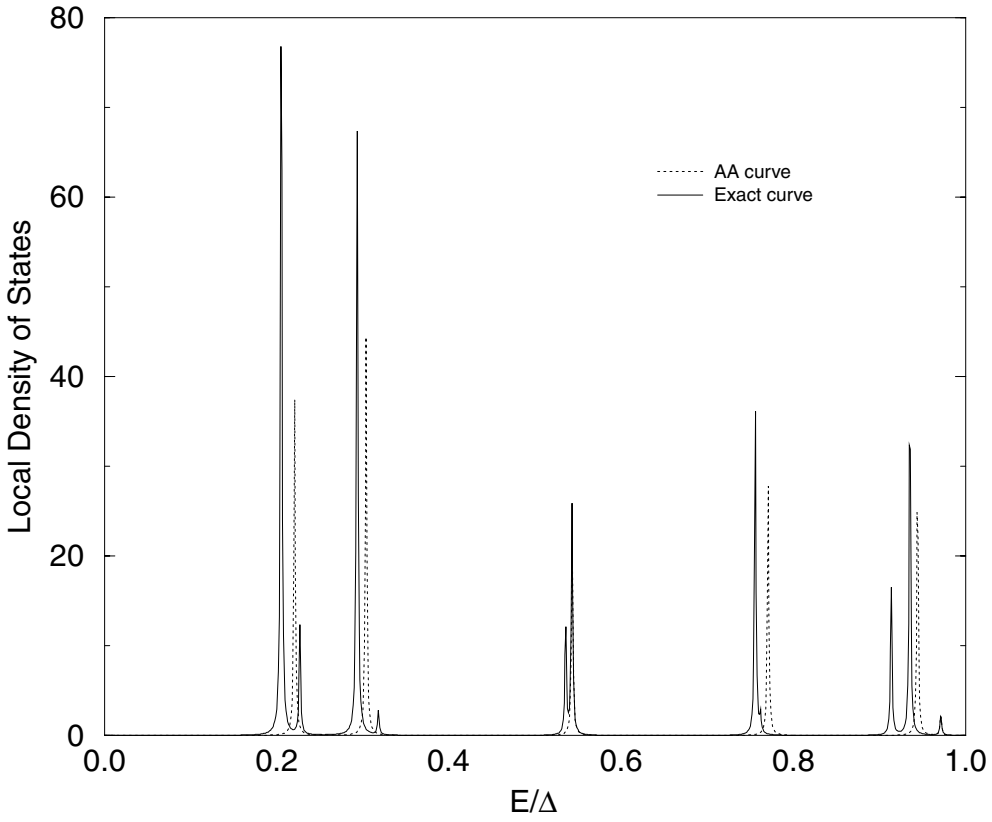

Figure 10. A plot of the LDOS against E/Δ, at $x = -1500$, for the SNSNS system depicted in figure 1, with $L_t = 4.4438$. The value of h is 0.25. Both the exact results and the ones within the Andreev approximation (AA) are shown.

of the state functions. For the exact solution the state functions are the even and odd, cosine and sine functions [7]. In the AA one just encounters plane waves, leading to equal height of the AA peaks. The exact LDOS for another position shows a different distribution of peak heights.

In figure 10 the LDOS is shown for an SNSNS junction having the smaller transverse width of $L_t = 4.4438$.

In view of this, only the (0, 0), (0, 1), and (1, 0) modes can propagate. The interfaces are chosen as indicated in the lower panel of figure 1. Although the superconducting layer in the middle has the same metallic properties as the superconductors forming the junction, due to the proximity effect one expects a gap value $h\Delta$ with $h < 1$, which will be confirmed by the self-consistent calculation to be presented in the following section. It is instructive to compare figure 10 with figure 11, calculated for the same configuration, but with $h = 0$. As we should, we found the same figure for the SNS system, because $h = 0$ implies absence of the middle superconducting sheet. In figure 11 only the exact states are shown, but with a value for δ which is negligible. Note the much larger scale for this very small δ. Compared to this figure, the lower states in figure 10, and particularly the state which lies below the gap value of 0.25Δ, are pushed up. Because Andreev states behave as v_F/L, v_F being the Fermi velocity, one would expect a rise by a factor of 4. In the following section we will show that the two N parts of the junction are not uncoupled yet, so the rise is somewhat smaller.

Now we turn to the self-consistent calculation of the gap Δ.

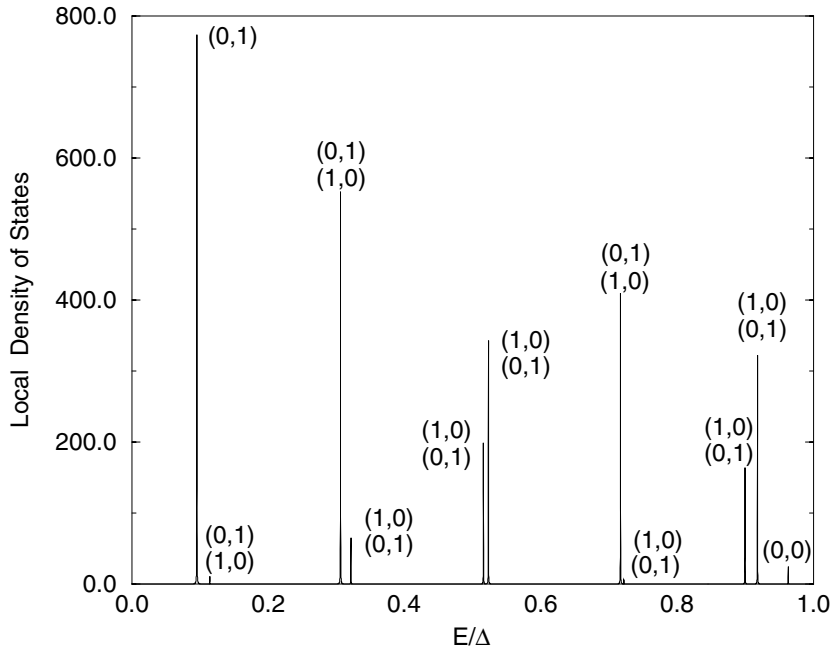

Figure 11. The LDOS against E/Δ at $x = -1500$, for an SNSNS system in which $L_t = 4.4438$ and $h = 0$.

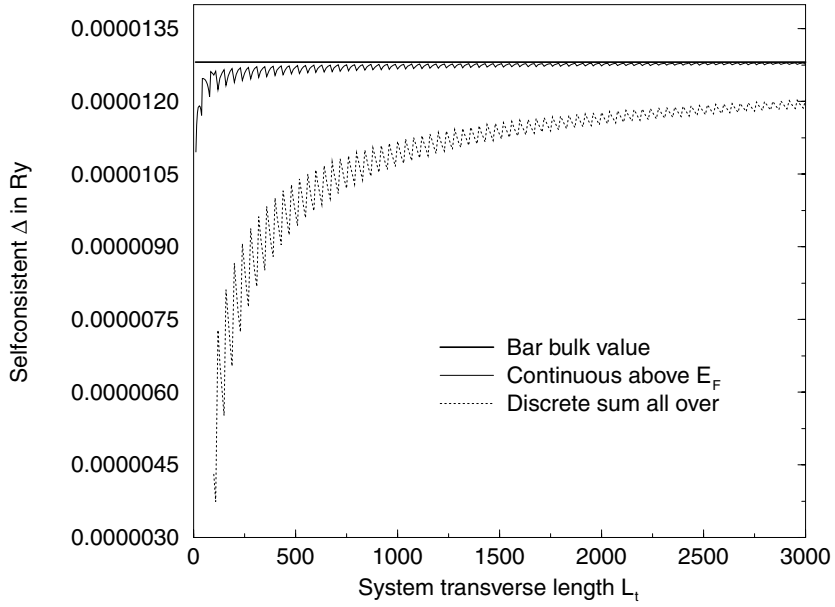

Figure 12. The self-consistent gap for a bar-shaped superconductor of macroscopic length in one direction, and with a finite transverse width L_t. The summations over the transverse wave vectors k_y and k_z have been carried out in a semicontinuous way for the solid curve, and in a rather coarse-grained way for the dotted curve. The limit for $L_t \to \infty$ is given by the constant bold line.

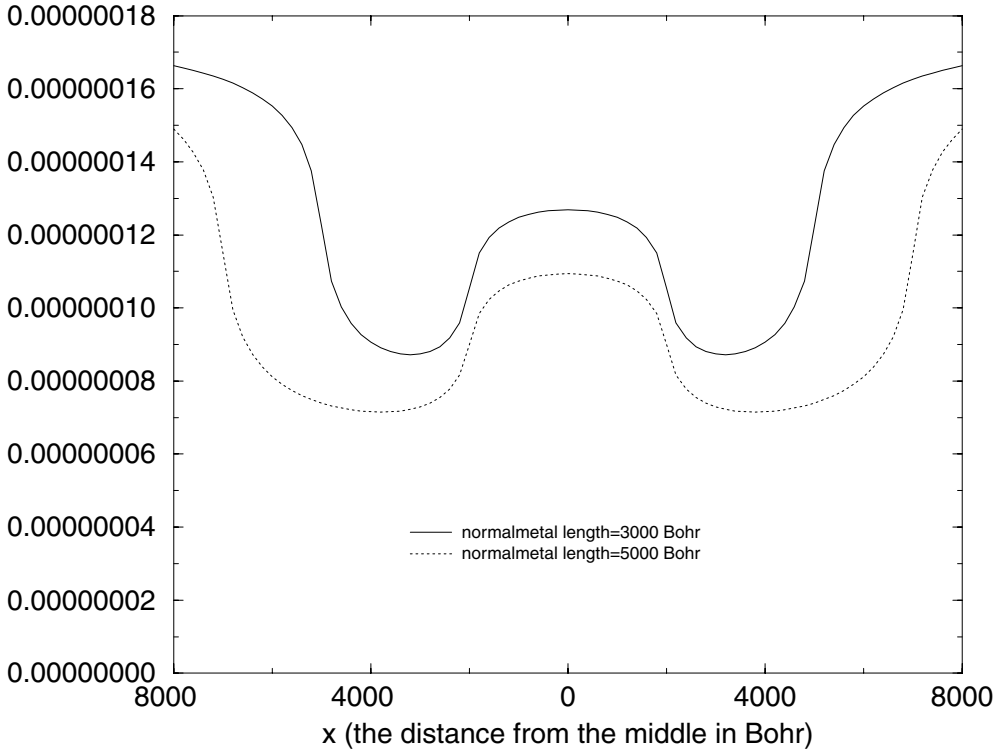

Figure 13. The pair amplitude against the distance from the middle, which is chosen at $x = 0$, of an SNSNS system with a transverse width $L_t = 100$. The interfaces are chosen at $x = \pm 2000, \pm 5000$ for the solid curve and $x = \pm 2000, \pm 7000$ for the dotted curve.

8. Self-consistent calculation of the gap

Using the self-consistency condition (6) for a bar-shaped superconductor, for which $A_t = L_y L_z$, we first calculated the gap Δ for an infinite homogeneous superconducting bar. Looking at the two systems depicted in figure 1, it is clear that the gap value found in that way must be the value for the outer superconducting parts of both junctions. After that one has to determine the gap value of the middle layer in the SNSNS junction. Depending on how one carries out the summation over the transverse wave vectors k_y and k_z, one obtains the upper or lower curve in figure 12. The bold line lies at the gap value for a bar superconductor with infinite width L_t, and so at the bulk value, to which the finite-bar gap values should converge. The oscillations in the solid and dashed curves come from the summation over discrete values of k_y and k_z. The dashed curve results from a summation over the entire range of the transverse wave vectors, in which also a cut-off at 3μ is applied, to which the results are not very sensitive. The mesh used has the spacing π/L_t. But it appears that the result is very sensitive to how the summation crosses the Fermi energy μ. The solid curve is obtained by summing up to just below μ, and by replacing the rest of the sum by the corresponding integral. We believe that the true behaviour lies in between the two curves, but somewhat closer to the solid curve than to the dashed curve. For both curves it holds that on decreasing the width L_t, superconductivity is suppressed.

Using the self-consistent gap value for the outer superconductors, one can calculate the self-consistent gap value for the superconducting layer in the middle of the SNSNS junction considered. In figure 13 we display the pair amplitude $F(x) \equiv \Delta/V$, which can have a finite

value in the N regions as well. This is done for two system lengths, 10 000 Bohr and 14000 Bohr, and for $L_t = 100$ Bohr. The thickness of the central superconducting layer is in both cases 4000 Bohr. The self-consistency is obtained by averaging the x-dependent gap value in the middle and by using that constant in the next iteration, a method employed already by Tanaka and Tsukada [8]. In this figure the proximity effect is nicely illustrated. A finite pair amplitude is found in the N layers, and this amplitude decreases when the N layers become thicker.

Similarly, the pair amplitude in the middle superconductor is smaller for a larger separation from the outer superconductors caused by thicker N layers. In order to show this feature, we have chosen to display the pair amplitude, because the gap value in the N layers, having $V = 0$, vanishes, and the corresponding figure would have been less informative.

9. Conclusions

An expression was derived for the Gor'kov Green's function of an arbitrary layered structure composed of clean superconductors and ballistic metals. A multiple-scattering approach was developed, leading to an easily recognizable and flexible form of the Green's function. The formalism is exact, but results according to the Andreev approximation can be obtained as well. The formalism is applied to an SNS and an SNSNS junction, while the gap values have been obtained self-consistently. Proximity effects come out nicely. In addition, the breakdown of the Andreev approximation, mentioned by Kümmel [6] and illustrated by Šipr and Györffy [7], is shown convincingly for junctions having a critical transverse width.

Applications to other systems, such as a multilayer and current-carrying systems, are in preparation.

Acknowledgments

Part of this work was part of the research programme of the Stichting voor Fundamenteel Onderzoek der Materie (FOM), which is financially supported by the Nederlandse Organisatie voor Wetenschappelijk Onderzoek (NWO). The stay of one of us (RESO) at the Vrije Universiteit Amsterdam was made possible by the Netherlands University Foundation for International Cooperation (NUFFIC) through support from the Physics Development Project of the University of San Carlos in Cebu, The Philippines, a cooperation of the University of San Carlos and the Vrije Universiteit Amsterdam.

References

[1] Gor'kov L P 1960 *Sov. Phys.–JETP* **10** 998
[2] Bogoliubov N N, Tolmacher V V and Shirkov D V 1959 *A New Method in the Theory of Superconductivity* (New York: Consultants Bureau)
[3] Eilenberger G 1968 *Z. Phys.* **214** 195
[4] Andreev A F 1964 *Sov. Phys.–JETP* **19** 1228
[5] Ashida M, Aoyama S, Hara J and Nagai K 1989 *Phys. Rev.* B **40** 8673
[6] Kümmel R 1974 *Phys. Rev.* B **10** 2812
[7] Šipr O and Györffy B L 1996 *J. Phys.: Condens. Matter* **8** 169
[8] Tanaka Y and Tsukada M 1991 *Phys. Rev.* B **44** 7578
[9] Ishii C 1970 *Prog. Theor. Phys.* **44** 1525
[10] Blaauboer M, Koperdraad R T W, Lodder A and Lenstra D 1996 *Phys. Rev.* B **54** 4283
[11] Koperdraad R T W 1995 The proximity effect in superconducting metallic multilayers PhD Thesis Vrije Universiteit ch 6
This Thesis is available on request from the corresponding author, A Lodder.